International Journal of Recent Technology and Engineering (IJRTE)
ISSN: 2277-3878, Volume-8 Issue-3, September 2019

Optimization of Bend Cross Section for Reduction of Pressure Drop in Pipe

Mohit Kumar, V K Bajpai

Abstract: ***Liquid distribution system needs to be optimally designed for low-pressure drop to ensure low energy consumption by pump. There may be other constraints as well like, pressure handling capacity of few components of system may restrict maximum pressure gradient that may be allowed. For such systems, even a slight variation in the pressure drop of any component may not be acceptable. This may result in large increase in pressure drop of complete system. The proposed work presents numerical and experimental study of variations in the pressure drop due to the change in cross section of geometry at bend location in pipe. The numerical study has been done with the help of CFD simulation. Numerical results thus obtained have been validated with the experimental data.***

Keywords: CFD, Ovalisation, Secondary flow, Turbulence.

I. INTRODUCTION

It is frequently required to distribute the liquid in different parts of system with the help of Liquid Distribution System (LDS) (Fig 1) comprising of header manifolds, hose & pipe networks, with sensors and controlling devices. Each channel of LDS consists of several such components in series or parallel as per system flow requirement. Pressure drop of various elements depend on their geometry of cross sections, apart from other parameters like surface roughness, temperature etc. Flow distribution and overall pressure drop of LDS depends on contribution of each channel of LDS. Increase in pressure drop of components in series within any channel may considerably increase the total pressure drop of system.

Any deviation in cross section of bend due to manufacturing tolerances may have severe impact on pressure drop of system. The proposed work deals with numerical analysis and experimental validation of the impact of this deviation in cross section at bend location. During fabrication, it is extremely difficult to control the area of cross section as strictly circular at bend location and it generally is deformed to an oval shape. The proposed work evaluates impact of degree of ovalisation in cross section at bend location on pressure drop of a 90° bend. Effect of ovalisation is calculated for various values of Reynolds Number ($\mathbf{R_e}$). It is worth mentioning here that the manufacturing tolerances on dimensions at other locations of same or different components also have impact on the pressure drop. However, this is not the scope of proposed research work. Literature has been reviewed thoroughly, but effect of variations in cross section of pipe at bend location on pressure drop is not available. Some of these are summarized below.

Crawford NM et al. (2003) [3] had proposed a model for calculating the pressure drop for turbulent single-phase fluid flow around sharp 90° pipe bends. Authors have presented new empirical equation for calculation of pressure drop due to separation of flow. Crawford NM et al. (2007) [2] had proposed another empirical equation for bends of lower curvature ratios, where pressure drop due to separation were dominant. Crawford N et al. (2009) [1] had compared four different turbulence models in commercial code and found that RSM was best of these four. However, authors have reported that none of them was suitable for cases where high separation of flow is involved. Daneshfaraz R et al. (2018) [4] studied effect of constrictions upstream of bend with the help of numerical simulations. Authors observed that constrictions have high impact on velocity profile and results in increase of separation of flow. Gorman JM et al. (2018) [6] had studied effect of blockage upstream of bend on pressure drop and heat transfer. Authors reported pressure drop proportional to square of velocity and thus predicting flow separation. In few cases, backflow result in fluctuation of Nusselt number along the pipe. Dutta P et al. (2016) [5] had studied effect of Reynolds number on flow separation and reattachment. Authors noted that $\mathbf{R_e}$ impacts separation and reattachment point. Hellström LHO et al. (2013) [7] had investigated curvature-induced structures downstream of a 90° bend with proper orthogonal decomposition analysis. Authors reported that secondary motions downstream of bend are governed by swirl switching motion apart from dean motion. Kim J et al. (2014) [8] simulated the swirling secondary flow in the downstream of a pipe bend. Authors reported that RNG k-ε is better suited for such simulation. Swirling intensity was reported to decrease because of curvature of bend. Muzychka YS et al. (2009) [9] have provided model for predicting friction factor in non-circular geometry including elliptical shape. However, model was restricted to laminar flow, that too in straight pipe. Pipe bends and turbulence flow were not considered in the study. Noorani A et al. (2013) [11] simulated steady turbulent flow in straight and curved pipes for various Reynolds number and curvature ratio using direct numerical simulation (DNS). Authors reported fluid characteristics calculated with DNS, for validation of simpler turbulence model.

Manuscript published on 30 September 2019
* Correspondence Author
Mohit Kumar*, Research Scholar, NIT Kurukshetra, Haryana, 136119, India. Email: mkabcd@gmail.com
Prof. V K Bajpai, NIT Kurukshetra, Haryana, 136119, India. . Email: vkbajpai@yahoo.com

Authors also brought out the fact that k-ε is suitable for lower curvature ratios, whereas it may not be accurate for higher curvature ratios. Noorani A et al. (2015) [10] examined the flows in curved pipe for different Reynolds number.
Authors identified large-scale travelling structures, which results in redistribution of the mean flow in the circular cross section. This phenomenon leads to lower gradients at the wall compared to the laminar flow. Ono A et al. (2011) [12] conducted experiment with short and long elbow for understanding flow induced vibrations. Authors reported that flow separation region was generated constantly in short elbow while it was intermittent in long elbow. It was also observed that periodic change of direction of secondary flow affect the behavior of separation region near the inside wall. Röhrig R et al. (2015) [13] compared LES results with various RANS turbulence modelling results for turbulent flow through a 90^0 pipe elbow in a range of moderately high Reynolds numbers. Authors found that weakening and strengthening of Reynolds stress anisotropy was not captured by RANS models. LES was found to be better in solving these problems. Rup K et al. (2011) [14] studied theoretically and experimentally flow in square cross-sectioned bend. Authors noticed large accelerations near the inner wall and local vortices in the subarea near the outer wall of the bend. Pressure difference between corresponding points at inside and outside wall along bend were found to be constant, for wide range of turbulence intensity at inlet section. Sami S et al. (2004) [15] had studied the effect of separation distance between two and three successive 90^0 elbows. Authors found that, when separation is more than 20 times diameter of pipe, successive elbows have no coupling effect. SST turbulence model was reported to the one, closely simulating the experimental values. Shusser M et al. (2015) [16] studied laminar flow in pipe with sudden expansion followed by bend. Authors reported that for low Reynolds number effect of sudden expansion dies soon and reattachment length is same for curve and straight path. However, for high Reynolds number inner vortex thickness could be considerable. These vortex results in different reattachment length along pipe circumference. Authors developed the reattachment length correlations. Reattachment length was reported as logarithmically dependent on the Reynolds number and linearly on the expansion ratio. Spalart PR et al. (2018) [17] had studied turbulence in non-circular ducts. Authors had developed empirical relationship for skin friction, but authors suggest verifying results with experiments as simulation used was done on models with similar assumptions as theory, and hence are in any case expected to correlate well. Taguchi S et al. (2018) [18] studied experimentally the Mass and momentum transfer characteristics in a 90° elbow. Authors reported increase in the mass transfer coefficients in the first half and a decrease in the second half of the inner wall of elbow with increasing Reynolds number. Tanaka M et al (2009) [19] developed customized code based on LES for simulation of flow structure in pipe elbow. Authors compared the results of software with experimental values and reported that reproduction of the unsteady motion in the elbow determines the accuracy of numerical simulation. Tanaka M et al. (2012) [20] studied the unsteady flow behavior through the short-elbow for different pipe diameters and curvature radius at various Reynolds number. Authors reported that secondary flow development and the flow separation formation in the elbow were dependent on velocity profile in upstream of the elbow and the curvature radius. Zhang H et al. (2013) [21] had numerically studied the pressure distribution and flow characteristics of curved pipes and elbows for Newtonian fluids. Authors reported the variation of pressure along circumference and along concave and convex side of bend. Zhang T et al. (2015) [22] studied the structural vibration and fluid borne noise through a 90^0 pipe elbow for turbulent flow. Authors simulated placement of guide vanes at various location using Fluid structure interaction and reported that at particular position, guide vanes can reduce vibrations. Pressure drop increased marginally with increased $\mathbf{R_e}$. Empirical relationship for Flow parameters including friction factor for non-circular duct had been proposed earlier [23]. However, empirical relationship was presented only for laminar flow regime in a straight duct. Model proposed by the authors, required only two parameters, first being aspect ratio of duct and second dimensionless duct length in contrast to three as reported earlier [24]. Authors had also reported that square root of area of cross section suits better to estimate the characteristic length scale of straight duct instead of hydraulic diameter. However, they did not consider the turbulence regime and effect of bend. Existing empirical correlations have been compared with experimental results for a small diameter bend [25]. Authors have used two-phase flow of fluid and reported that most of empirical correlations are not versatile and can deal with a small range of diameters only. Authors also proposed a new empirical correlation, which predicts well, for an entire range of parameters proposed by them. Calculations of frictional pressure drop and effect of sharp bends, up and downstream for two-phase flow has been carried out and compared with experimental results [26]. Authors had reported that the effect of bend was observed towards its downstream.
In all the above reported research works, efforts were done to study the effect of ideal bends at its location and near its vicinity. Lot of research work had been carried out in related areas, but the effect of change of bend circular cross section to oval shape of random dimension on pressure drop has not been reported. This type of research study requires concentrated efforts on performing multiple iterations of fluid flow characteristics for a large range of input variables. The proposed research work takes into account variation in cross section at bend locations and $\mathbf{R_e}$. The other variables like, fluid properties, fluid phase are held as constant.
For a practical engineering application, this type of analysis of pressure drop is possible by simplifying the problem in hand and use of CFD analysis. In this respect, the CFD results have been compared with the empirical correlations available in literature [12] and authors drew conclusion, that CFD codes are highly accurate and, on several occasions, can resolve sensitivity to intricate geometrical variations even better than the empirical formulas.

II. APPLICATION IN SYSTEM

LDS (Fig 1) is required to be designed for a low pressure drop in a system, which is proposed to be installed on rotating platform. Rotary joint, which supplies the coolant (water) from stationary part to the rotating part, is having a fixed capacity in terms of pressure it can handle.

This defines the constraint on overall pressure drop that can be allowed in the system. Therefore, control of deviation in value of pressure drop from designed values, for each component of LDS is required.

The designer needs to set up a standard procedure for tuning different flow rates in different channels of a LDS. This requires knowledge of tolerances on pressure drop values. Further, unusual and random pressure drops because of manufacturing variations may induce additional pressure drop in system due to extra tuning requirements. In extreme cases, getting desired flow rate distribution may not be possible.

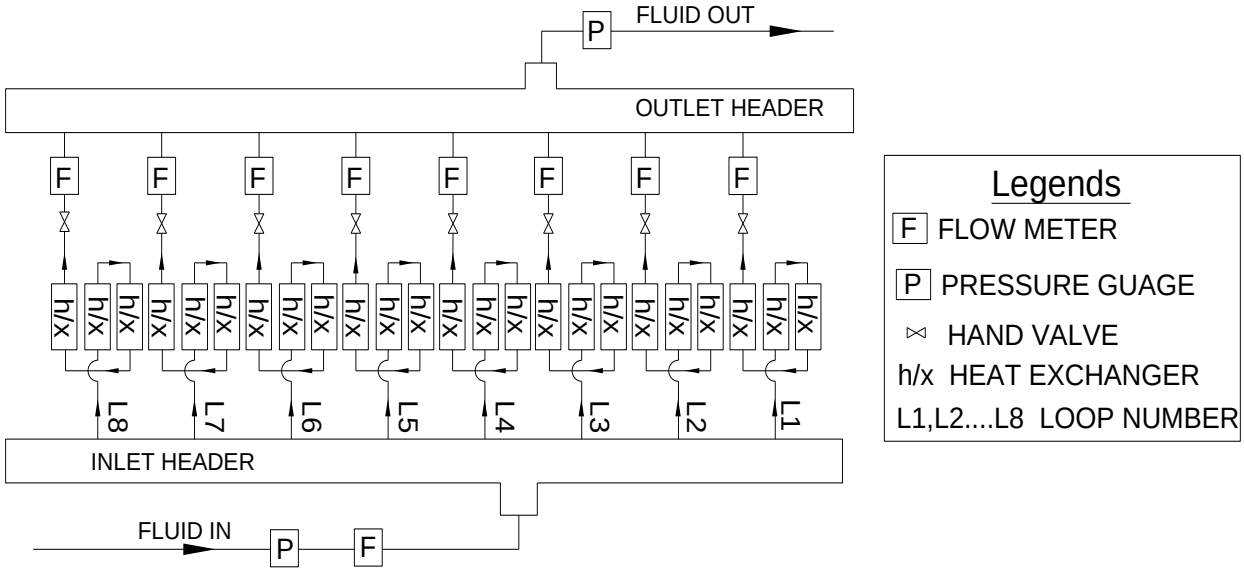

Fig. 1. Liquid distribution system (LDS)

III. NUMERICAL SIMULATION

A. Modeling of Geometry of Bend Cross Section

Ideally, cross section of a bend throughout its length should be circular (or near circle) (Fig 2). However, during bending process, cross section decreases in the radial direction along axis joining intrados to extrados of the bend and increases along axis perpendicular to it (Fig 3). Ovalisation of bend cross section can be approximated with an elliptical shape with a good accuracy level. This shape correlates well with the physically measured shape, and same has been used in the work presented in this paper. Practically because of various reasons like improper diameter to thickness ratio, heterogeneous material or ellipticity in inner and outer cylinder of pipe, ratio of pipe diameter to bend radius etc., and bends may take different shapes of cross section. Bends with this type of manufacturing defects are easy to identify and can be rejected, as they can be identified visually. Proposed work does not include such type of defects. In addition, extreme cases of aspect ratio (major to minor axis) of elliptical cross section may not be possible in a practical scenario. In the proposed work, experimental verification of these zones has not been carried out, as actual bend's geometry will be widely different from elliptical cross section. Hence, experimental results are not expected to correlate well for these cases. However, only for academic interest, results for elliptical ovalisation have been calculated and presented with extreme possible values with simulation.

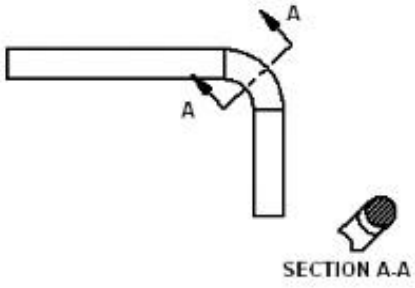

Fig. 2.Bend with perfect circular cross section

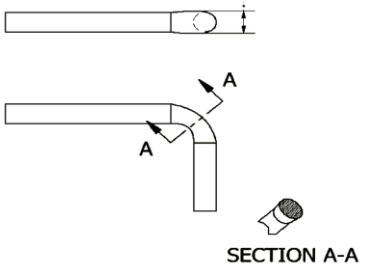

Fig. 3.Bend with elliptical cross section

B. Assumptions

It has been assumed that circular cross section becomes elliptical after bending operation during fabrication, and perimeter of ellipse is same as that of the original circular cross section of bend (1).

$$\mathbf{p} = 2\,\pi\,\{(\mathbf{a}^2+\mathbf{b}^2)/2\}^{1/2} = 2\,\pi\,\mathbf{r} \qquad (1)$$

where,

p = Perimeter of ellipse
a = Minor axis radius (half diameter) of ellipse
b = Major axis radius (half diameter) of ellipse
r = radius of circular cross section, when there is no ovalisation of bend cross section

Since **p** remains constant, 'a' becomes dependent variable. Therefore, instead of ellipticity, **b** (major axis radius) of ellipse alone is used to measure degree of ovalisation.

C. CFD Turbulence Simulation Model

CFD simulation model capable of modelling both boundary layer and free stream conditions properly was required for the proposed work. Menter et al. [26] had proposed improved variant of popular k-ω model, viz k-ω-SST, which is most suitable for this purpose.

Shear stress transport (SST): In SST model, k-ε equation is first transformed to k-ω formulation. Blending function (F), is multiplied to original k-ω formulation and (1-F) is multiplied to transformed k-ε equation, both equations are then added together. Design of blending function is such that its value is '1' in sublayer & logarithmic region and it gradually reduces to zero in wake region of boundary layer. This ensure that, multiple of k-ω becomes zero in wake region of boundary layer & free-stream, and that of k-ε becomes zero in near wall region. SST models transport of shear stress like in full Reynolds stress model (RSM) in adverse pressure gradient condition and switches back to original eddy viscosity model in free shear layers. This is done by using similar blending function as used in main equations. This model is best suitable for present study because of its versatility in wide variety of flow conditions. Limitation of k-ω SST model is that, it requires small Y+ values (less than '1'). This requires very fine mess and may considerably increase the computation time. However, looking at versatile nature for dealing with large range of variations in flow characteristics, this model is used for present work. This model being popular CFD model is readily available in commercial CFD code. Instead of solving the equations numerically, commercially available solver viz Ansys Fluent has been used.

IV. EXPERIMENTATION

Experimental verification has been carried out with the help of a test jig (Fig 4). The test jig consists of motor, reservoir for fluid (water), control valves and flow meter. The flow rate can vary from 0-40 litre/minute on a 3/8 inch BSP (British standard pipe) standard hose. The variation of flow rate was carried out with the help of a by-pass loop. Both, the main loop and the by-pass loop have control valves to regulate the fluid flow rate. Main loop's flow rate can be read easily by a flow meter. Test jig was used to calculate pressure drop across bend, with the help of pressure gauge at both inlet and outlet.

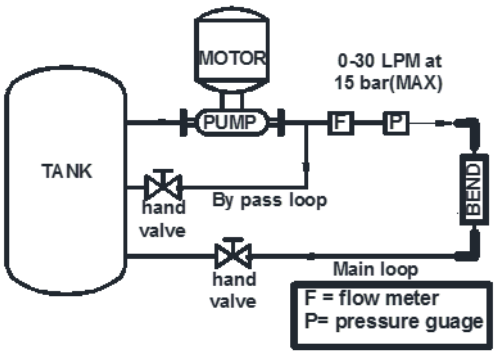

Fig. 4.Schematic diagram of Test jig

V. RESULTS AND DISCUSSION

Nomenclature used here for reference planes had been shown in Fig 5

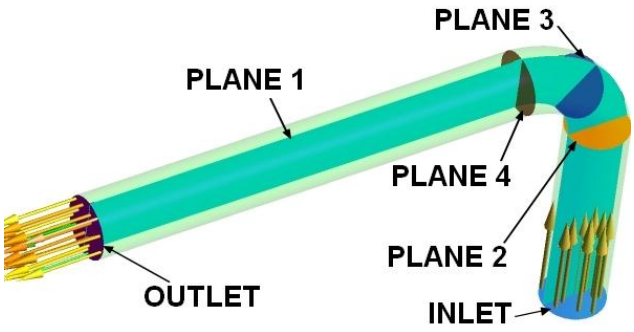

Fig. 5. Geometry of bend showing nomenclature as referred in text

A. Numerical simulation observations

Cross section of an ideal bend is circular across entire length. Hence, there is no convergence or divergence across bend due to change in area or shape of cross section. Secondary flow is only because of bend. Geometry of bend with ellipticity is such that, (a) Across, vertical mid plane (Plane 1), pipe cross section decreases from start of bend (Plane 2) to mid of bend (Plane 3) and then increases from there to end of bend (Plane 4). (b) For surfaces running parallel to mid line, cross section increases from Plane 2 to Plane 3 and then start decreasing until Plane 4. This creates fluid to converge and then diverge across Plane 1 and vice-versa, across surfaces parallel to mid line. Planes and surfaces adjacent to Plane 1 and bend mid line observes similar behavior with magnitude proportional to cross section decrease or increase. This phenomenon can be easily visualized in streamline plot (Fig 6) and vector plot of velocity at Plane 3 (Fig 7) and Plane 4 (Fig 8).

Irrespective of bend cross section, fluid separation near inside wall of bend and in vicinity of Plane 4 is observed due to upstream bend (Fig 9).

Retrieval Number C4897098319/2019©BEIESP
DOI: 10.35940/ijrte.C4897.098319
Journal Website: www.ijrte.org

Published By:
Blue Eyes Intelligence Engineering
& Sciences Publication

Velocity plot (Fig 10) on Plane 1, Plane 3 and Plane 4 shows low velocity in this region. In addition to this, in case of bend with ellipticity, at the end of the bend (Plane 4) fluid converges from sides (across surfaces parallel to bend mid-line) towards center of pipe due inertia fluid carries from diverging zone as explained above (Fig 6). Further, due to reduction of height of pipe at Plane 3, higher degree of squeezing of fluid towards center of pipe is observed. These combined effect results in increase of secondary flow and higher turbulence at center of pipe (Fig 11). A similar trend is observed for all $\mathbf{R_e}$ under considerations, with difference of, increase in magnitude.

Pressure drop is plotted against **b** of elliptical cross section of bend (Fig 12). Fig 13 shows percentage increase of pressure drop versus ellipticity of cross section. For simulated pipe with a diameter 6.5 mm, a perfect circle is denoted by an ellipse with **a** = **b** = 3.25(= 6.5/2) mm. Pressure drop corresponding to **b** = 3.25 mm (perfect circle) was taken as reference to measure deviation (percent error) of pressure drop in ovalized cross section of bend. Hence, % increase of pressure drop is evaluated as

$$\% \text{ increase of pressure drop} = (\Delta P_i - \Delta P_{sc})/ \Delta P_{sc} \times 100$$

Where,

ΔP_i = Pressure drop for i^{th} data point. Each data point represents different value of b

ΔP_{sc} = Simulated pressure drop of bend for circular cross section

Value of maximum tolerance that can be allowed on ellipticity, for a required tolerance on pressure drop can be directly recorded from graph. For example, if maximum tolerance allowed on pressure drop is 10% of ΔP_{sc}, major radius of elliptical cross section of bend, **b** < 3.8 mm.

B. Summary of observation based on numerical simulation:

i. Fig 12 shows that, pressure drop increases non-linearly with ellipticity of bend cross section geometry.
ii. Fig 13 also shows that, if **b** < 3.8 mm, increase in pressure drop is nearly 10 percent, for all values of $\mathbf{R_e}$ under consideration in study. After this point pressure drop increases rapidly with increase of ellipticity.
iii. Therefore, this threshold value can be used as optimal value of manufacturing tolerance. However, for different scenarios, value of tolerance can be relaxed or made more stringent to suit the accuracy requirement.

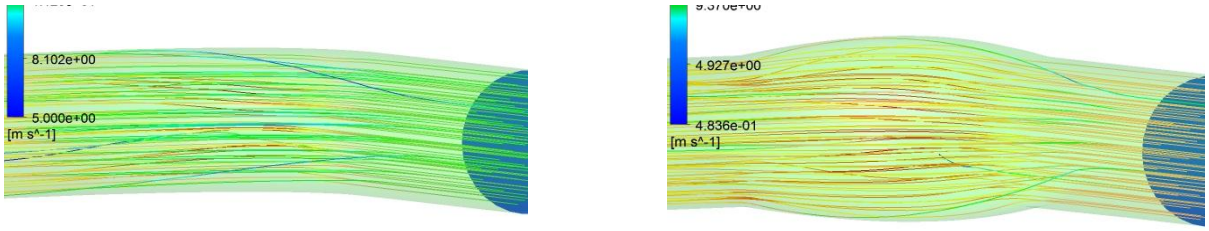

(a) For circular cross section (b) For elliptical cross section

Fig. 6.Top view of streamlines in bend

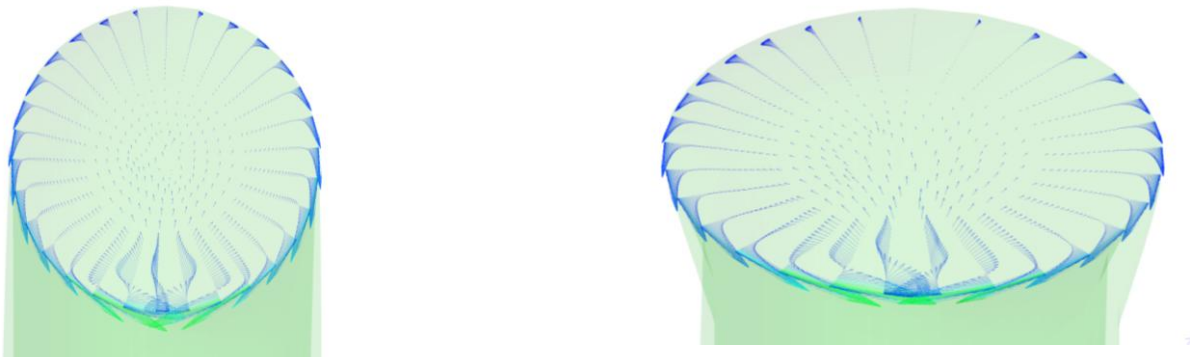

(a) For circular cross section (b) For elliptical cross section

Fig. 7.Vector plot of velocity at Plane 3

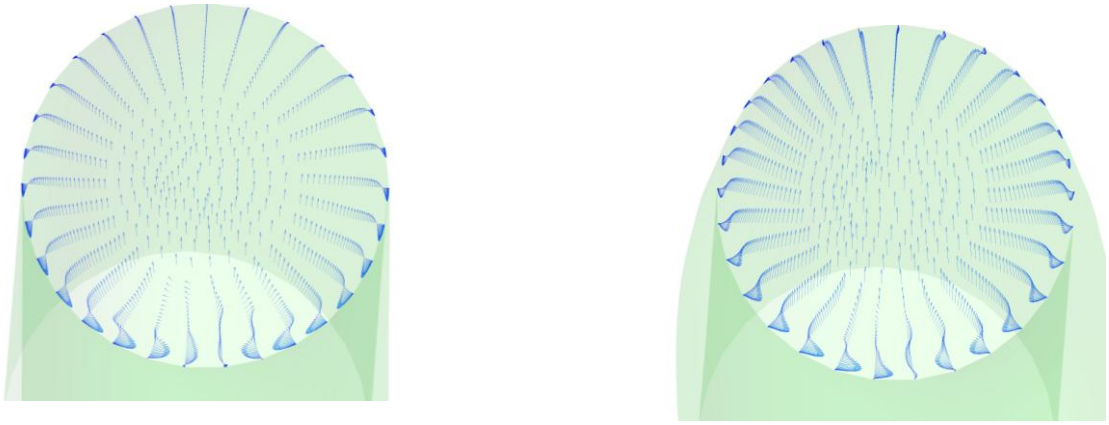

(a) For circular cross section (b) For elliptical cross section

Fig. 8.Vector plot of velocity at Plane 4

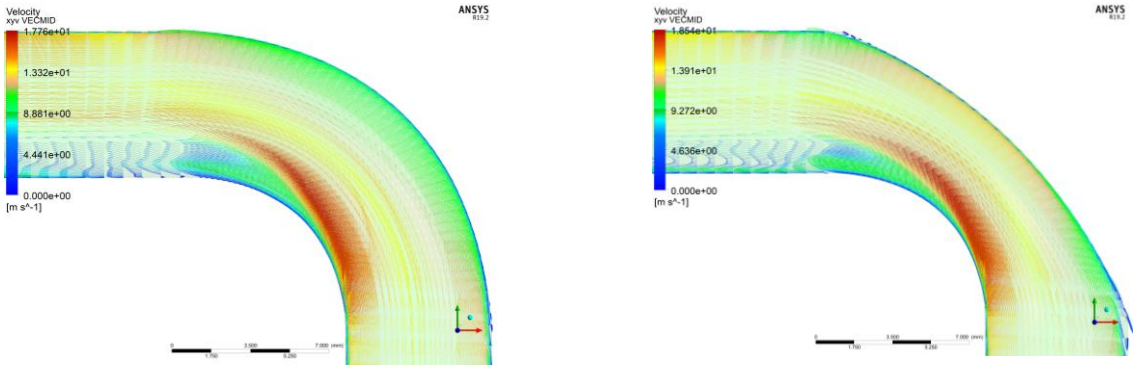

(a) For circular cross section (b) For elliptical cross section

Fig. 9.Vector plot of velocity at Plane 3

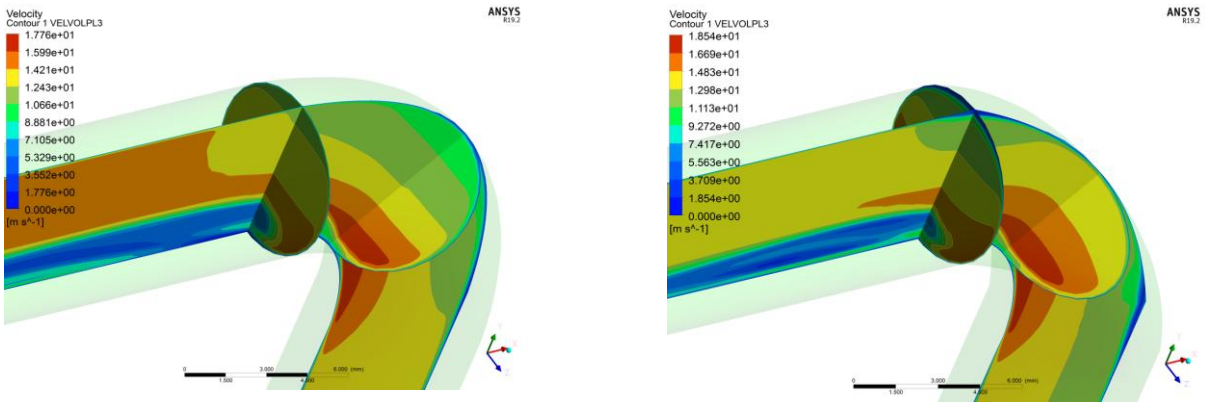

(a) For circular cross section (b) For elliptical cross section

Fig. 10. Velocity profile on Plane 1, Plane 3 and Plane 4

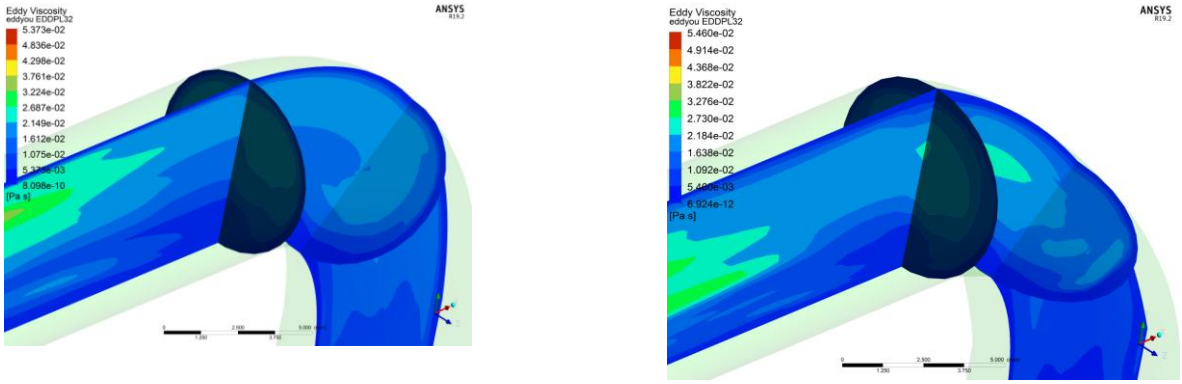

(a) For circular cross section (b) For elliptical cross section

Fig. 11. Eddy viscosity plot at Plane 1, Plane 3 and Plane 4

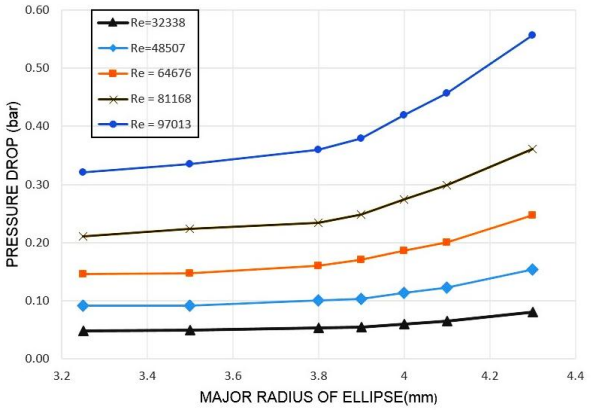

Fig. 12. Pressure drop for various bend cross sections at different R_e

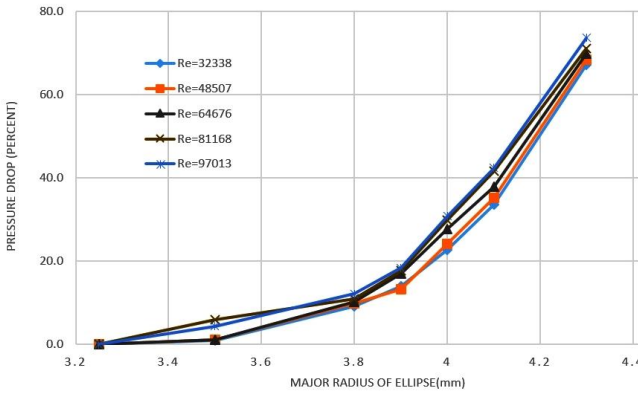

Fig. 13. Percent pressure drop for various bend cross sections at different R_e

C. Experimental validation of numerical simulation

Numerical simulation results have been compared with experimental values and are tabulated in Table I. Table I shows data for bend having Major axis radius, **b** = 4.0 mm

Notation:

Err = Error

ΔP_{ex} = Pressure drop measured experimentally

ΔP_{sc} = Simulated pressure drop of bend for circular cross section

ΔP_{so} = Simulated pressure drop of bend with ovalisation in cross section

Table I: Experimentally measured v/s simulated values

R_e	ΔP_{ex} (bar)	ΔP_{sc} (bar)	ΔP_{so} (bar)	E_{rr} in ΔP_{sc} (%)	Err in ΔP_{so} (%)
32338	0.21	0.18	0.19	14.3	9.5
48507	0.42	0.36	0.39	14.3	7.1
64676	0.73	0.62	0.66	15.1	9.6
81168	1.09	0.92	0.99	15.6	9.2
97013	1.64	1.34	1.48	18.3	9.8

Analysis of Table I reveals that, percent error has reduced to single digit value, when simulation is done with ellipticity of bend into consideration. This error was in double digit (upto 18.3%) when bend cross section was treated as perfect circle in simulation. For R_e = 97013 percent error in simulated results with elliptical cross section of bend is ≈ 50%, compared to those of circular cross section. Here point worth mentioning is that bends beyond certain threshold point (**b** > 3.8 mm) point have been eliminated. This is because they will induce very high pressure drop. Pipes with this type of bends are treated as defective and are rejected during the inspection, for practical engineering systems.

As expected, when ellipticity is included in simulated model, reduction in percent error of pressure drop, simulated versus experimentally measured value is observed, with increase in value of **b**. Percent errors are high for lower values of **b** and R_e. One reason behind this phenomenon is that CFD simulation has been optimized for lower computation cost. Accuracy level of simulation is kept to near second decimal place only. Overall pressure-drop for low values of **b** and R_e are of same order (second decimal place). Hence, CFD simulation error becomes appreciable percentage of pressure drop value. However, since absolute value of pressure drop is very low, it becomes insignificant for practical engineering systems. Therefore, increasing simulation accuracy at cost of time is not justifiable for these cases.

Considering above facts, it is thus evident that, there is significant advantage in terms of accuracy of CFD simulation when effect of ellipticity of cross section of bend is considered. This becomes increasingly important when several such bends are connected in series in individual channel of LDS (Fig 1).

VI. CONCLUSION

Convergence of fluid followed by divergence, is observed across all vertical planes of bend and vice-versa for surfaces running parallel to bend mid line. This results in increase of secondary flow and turbulence, giving rise to increase in pressure drop across bend.

Pressure drop values calculated with help of CFD simulation have been compared with experimental values and following conclusions can be drawn:

a. When proposed model with ovalisation of bend cross section considered is used in simulation, there is reduction in percent error of computed results with respect to experimentally measured values. In extreme cases, error of simulated results with elliptical bend cross section reduces to nearly half, compared to results obtained with circular bend cross section.

b. Pressure drop increases with increase in **b** (major axis radius of ellipse) of bend cross-section and is non-linear. Pressure drop increase is negligible until threshold value of **b** (≈ 3.8 mm). After this value of **b**, pressure drop rises sharply.

c. For range of $\mathbf{R_e}$ (32000 to 100000) under consideration, percent increase in pressure drop is function of ellipticity of bend cross section, but is independent of $\mathbf{R_e}$.

Hence, ovalisation effect considered in the simulation has resulted in considerable improvement in accuracy of results. An optimum value of ovalisation thus found results in considerable reduction of pressure drop without increasing manufacturing complexity.

REFERENCES

1. Crawford, N., Spence, S., Simpson, A., & Cunningham, G. (2009). A numerical investigation of the flow structures and losses for turbulent flow in 90 elbow bends. Proceedings of the Institution of Mechanical Engineers, Part E: *Journal of Process Mechanical Engineering*, 223(1), 27-44.
2. Crawford, N. M., Cunningham, G., & Spence, S. W. T. (2007). An experimental investigation into the pressure drop for turbulent flow in 90 elbow bends. Proceedings of the Institution of Mechanical Engineers, Part E: *Journal of Process Mechanical Engineering*, 221(2), 77-88.
3. Crawford, N. M., Cunningham, G., & Spedding, P. L. (2003). Prediction of pressure drop for turbulent fluid flow in 90 bends. Proceedings of the Institution of Mechanical Engineers, Part E: *Journal of Process Mechanical Engineering*, 217(3), 153-155.
4. Daneshfaraz, R., Rezazadehjoudi, A., & Abraham, J. (2018). Numerical investigation on the effect of sudden contraction on flow behavior in a 90-degree bend. *KSCE Journal of Civil Engineering*, 22(2), 603-612.
5. Dutta, P., Saha, S. K., Nandi, N., & Pal, N. (2016). Numerical study on flow separation in 90 pipe bend under high Reynolds number by k-ε modelling. Engineering Science and Technology, *an International Journal*, 19(2), 904-910.
6. Gorman, J. M., Sparrow, E. M., Smith, C. J., Ghosh, A., Abraham, J. P., Daneshfaraz, R., & Rezazadeh Joudi, A. (2018). In-bend pressure drop and post-bend heat transfer for a bend with a partial blockage at its inlet. *Numerical Heat Transfer*, Part A: Applications, 73(11), 743-767.
7. Hellström, L. H., Zlatinov, M. B., Cao, G., & Smits, A. J. (2013). Turbulent pipe flow downstream of a $90 {{}^\circ} $ bend. *Journal of Fluid Mechanics*, 735.
8. Kim, J., Yadav, M., & Kim, S. (2014). Characteristics of secondary flow induced by 90-degree elbow in turbulent pipe flow. *Engineering Applications of Computational Fluid Mechanics*, 8(2), 229-239.
9. Muzychka, Y. S., & Yovanovich, M. M. (2009). Pressure drop in laminar developing flow in noncircular ducts: A scaling and modeling approach. *Journal of Fluids Engineering*, 131(11), 111105.
10. Noorani, A., & Schlatter, P. (2015). Evidence of sublaminar drag naturally occurring in a curved pipe. Physics of Fluids, 27(3), 035105.
11. Noorani, A., El Khoury, G. K., & Schlatter, P. (2013). Evolution of turbulence characteristics from straight to curved pipes. *International Journal of Heat and Fluid Flow*, 41, 16-26.
12. Ono, A., Kimura, N., Kamide, H., & Tobita, A. (2011). Influence of elbow curvature on flow structure at elbow outlet under high Reynolds number condition. *Nuclear Engineering and Design*, 241(11), 4409-4419.
13. Röhrig, R., Jakirlić, S., & Tropea, C. (2015). Comparative computational study of turbulent flow in a 90 pipe elbow. *International Journal of Heat and Fluid Flow*, 55, 120-131.
14. Rup, K., & Sarna, P. (2011). Analysis of turbulent flow through a square-sectioned duct with installed 90-degree elbow. *Flow Measurement and Instrumentation*, 22(5), 383-391.
15. Sami, S., & Cui, J. (2004). Numerical study of pressure losses in close-coupled fittings. *HVAC&R Research*, 10(4), 539-552.
16. Shusser, M., Ramus, A., & Gendelman, O. (2016). Flow in a Curved Pipe With a Sudden Expansion. *Journal of Fluids Engineering*, 138(2), 021203.
17. Spalart, P. R., Garbaruk, A., & Stabnikov, A. (2018). On the skin friction due to turbulence in ducts of various shapes. *Journal of Fluid Mechanics*, 838, 369-378.
18. Taguchi, S., Ikarashi, Y., Yamagata, T., Fujisawa, N., & Inada, F. (2018). Mass and momentum transfer characteristics in 90° elbow under high Reynolds number. *International Communications in Heat and Mass Transfer*, 90, 103-110.
19. Tanaka, M. A., Ohshima, H., & Monji, H. (2009, January). Numerical investigation of flow structure in pipe elbow with large eddy simulation approach. *In ASME 2009 Pressure Vessels and Piping Conference* (pp. 449-458). American Society of Mechanical Engineers.
20. Tanaka, M., & Ohshima, H. (2012). Numerical investigation on large scale eddy structure in unsteady pipe elbow flow at high Reynolds number conditions with large eddy simulation approach. *Journal of Power and Energy Systems*, 6(2), 210-228.
21. Zhang, H., Zhang, X., Sun, H., Chen, M., Lu, X., Wang, Y., & Liu, X. (2013). Pressure of Newtonian fluid flow through curved pipes and elbows. *Journal of Thermal Science*, 22(4), 372-376.
22. Zhang, T., Zhang, Y. O., & Ouyang, H. (2015). Structural vibration and fluid-borne noise induced by turbulent flow through a 90 piping elbow with/without a guide vane. *International Journal of Pressure Vessels and Piping*, 125, 66-77.
23. Muzychka, Y. S., & Yovanovich, M. (1998, June). Modeling friction factors in non-circular ducts for developing laminar flow. *In 2nd AIAA, Theoretical Fluid Mechanics Meeting* (p. 2492).
24. Shah, R. K. (1978). A correlation for laminar hydrodynamic entry length solutions for circular and noncircular ducts. *Journal of Fluids Engineering*, 100(2), 177-179.
25. Autee, A. T., & Giri, S. V. (2016). Experimental study on two-phase flow pressure drop in small diameter bends. *Perspectives in Science*, 8, 621-625.
26. De Kerpel, K., De Schampheleire, S., De Keulenaer, T., & De Paepe, M. (2016). Effect of the bend geometry on the two-phase frictional pressure drop and flow behaviour in the vicinity of the bend. *Applied Thermal Engineering*, 104, 403-413.
27. Menter, F. R. (1994). Two-equation eddy-viscosity turbulence models for engineering applications. AIAA journal, 32(8), 1598-1605.
28. Rumsey, C. L. (2007). Apparent transition behavior of widely-used turbulence models. *International Journal of Heat and Fluid Flow*, 28(6), 1460-1471.

AUTHORS PROFILE

Mohit Kumar is currently a Research scholar in N.I.T. Kurukshetra, Haryana, India. He is working as Manager in R&D department of BEL, Ghaziabad, A Govt of India, Ministry of Defence Entp. He had passed his M.Tech degree in Mechanical Engg from NIT Kurukshetra, Haryana. His areas of interest are: **Current interest**: Design and thermal analysis for air as well as liquid cooled electronics enclosures for Radars and Satellite communication equipment.

Research Activities: Liquid cooling for large size antennas for Radar applications. Thermal management of Satellite communication equipment.
Future plans: Wind load analysis for reflector type antenna systems and composite Radomes, using coupled analysis of CFD and FEA. Conversion of liquid cooled systems to air cooled systems.

Dr VK Bajpai is currently working as Professor in National Institute of Technology, Kurukshetra, Haryana, 136119 India. He is Ph.D In Thermal Engineering. His Area of Interest are:
Current interest: Renewable energy resources, Heat Transfer, Refrigeration and air conditioning, Thermodynamics, IC Engines and gas turbines, Fluid Engineering, Steam and Power generations.
Research Activities: Use of solar energy in HVAC is being explored. Regeneration of Desiccant wheel by solar energy and optimization of its different parameters.
Future plans: Planning to have a project on solar energy from MNRE and planning to develop Centre of excellence in Renewable Energy Sources in the Institute.